

Robust a-posteriori error estimates for weak Galerkin method for the convection-diffusion problem

Natasha Sharma^{a,*}

^a*Department of Mathematical Sciences, University of Texas of El Paso, El Paso, TX 79968*

Abstract

We present a robust a posteriori error estimator for the weak Galerkin finite element method applied to stationary convection-diffusion equations in the convection-dominated regime. The estimator provides global upper and lower bounds of the error and is robust in the sense that upper and lower bounds are uniformly bounded with respect to the diffusion coefficient. Results of the numerical experiments are presented to illustrate the performance of the error estimator.

Keywords: weak Galerkin, finite element methods, discrete weak gradient, *a posteriori* error estimates, convection-diffusion equation, adaptive mesh refinement

1. Introduction

We consider the following convection-diffusion equations as our model problem

$$-\operatorname{div}(\varepsilon \nabla u) + \operatorname{div}(\mathbf{b}u) + au = f \text{ in } \Omega, \quad (1.1a)$$

$$u = 0 \text{ on } \Gamma, \quad (1.1b)$$

where Ω is a polygonal domain in \mathbb{R}^2 with boundary Γ and where the data of the problem (1.1) and the right-hand side in (1.1a) satisfy the following assumptions:

A1. $\varepsilon > 0$.

*Corresponding author

Email address: nssharma@utep.edu (Natasha Sharma)

A2. $f \in L^2(\Omega)$, $\mathbf{b} \in W^{1,\infty}(\Omega)^2$, $a \in L^\infty(\Omega)$.

A3. There exists a positive constant c_0 such that

$$0 < c_0 \leq \frac{1}{2} \operatorname{div} \mathbf{b} + a \quad \text{on } \Omega. \quad (1.2)$$

One of the challenges in the numerical approximations to (1.1) is that when the problem is convection-dominated, the solutions to these problems possess layers of small width. In the presence of these layers, the solutions and/or their gradients change rapidly and as a consequence, standard finite element methods give inaccurate approximations unless the mesh size is fine enough to capture the layers.

In response to this challenge, several numerical approaches have been proposed over the years including stabilized methods [1, 2, 3, 4, 5], discontinuous Galerkin (DG) methods [6, 7, 8, 9, 10, 11, 12, 13, 14, 15] and most recently, the weak Galerkin (WG) methods [16, 17]. In particular, the WG methods use discontinuous approximations and have gained popularity owing to their attractive properties such as mass conservation, flexibility of geometry, flexibility on the choice of approximating functions [18]. It is interesting to note that over and above the advantages enjoyed by WG methods, the additional advantages of the WG scheme proposed in [17] is that it assumes a simple form and does not require any strict assumptions on the convection coefficient, a requirement which is crucial for several of the existing methods such as [8, 13, 14, 16]. Additionally, this simple WG scheme converges at the rate of $\mathcal{O}(h^{k+1/2})$ in the strongly advective regime, k here denoting the polynomial order.

The motivation of our paper stems from the fact that despite the advantages of this simple WG scheme, it exhibits a poor performance in the intermediate regime see [17, Example 2], for instance. Our goal in this paper is to present a posteriori error analysis for the simple WG method proposed in [17]. We further demonstrate that by relying on adaptively refined meshes based on a posteriori residual-type estimator, we can retrieve the optimal order of convergence for all the regimes not just the convection-dominated regime. Additionally, we also prove that this estimator provides global upper and lower bounds of the error and is robust in the sense that upper and lower bounds are uniformly bounded with respect to the diffusion coefficient.

Existing literature for convection-diffusion problems solved using adaptive finite element methods based on a posteriori error estimates was initialized

by Eriksson and Johnson in [19] and enriched by several works authored and co-authored by Verfürth in [20, 21, 22]. Within the DG framework, a posteriori estimates were developed by Schötzau and Zhu in [13, 14], and by Ern and co-authors in [23, 24]. In [15], a posteriori analysis using the hybridizable DG (HDG) method was presented and the error analysis relies on the extra conditions imposed on the convection coefficient. Furthermore, the proof of the local efficiency of the error estimator explicitly imposes a condition on mesh size to prove local efficiency see [15, Lemma 5.3].

The WG method was originally introduced in [18] by Wang and Ye as a class of finite element methods that employ weakly defined differential operators to discretize partial differential equations without demanding any fine tuning of parameters in its weak formulation. While much attention has been paid to developing weak Galerkin methods for a wide class of problems [25, 26, 27, 28, 29, 30, 31, 32, 33], there is not much development in the direction of adaptive WG methods and most of the existing a posteriori error analysis is derived for either the second-order elliptic equations [34, 35, 36, 37] or for the Stokes problem [38].

The paper is organized as follows. Section 2 develops the weak Galerkin finite element method for the model problem. Section 3 derivation of the a posteriori error analysis is presented. Section 4 demonstrates the effectiveness of our method with results of numerical experiments.

2. Weak Galerkin Formulation

Let $\{\mathcal{T}_h\}_{h>0}$ be a uniformly shape-regular partition of Ω into rectangular or triangular cells. For any $T \in \mathcal{T}_h$, let h_T denote the diameter of T , $h = \max_{T \in \mathcal{T}_h} h_T$, the mesh size of \mathcal{T}_h and ∂T denote the boundary of T .

Let \mathcal{E}_h and $\bar{\mathcal{E}}_h$ denote the collection of all the interior edges and all the edges associated with the triangulation \mathcal{T}_h respectively. Also, for any $E \in \bar{\mathcal{E}}_h$, let h_E denote the length of E . We assume that there exists a constant $\kappa > 0$ such that for each $T \in \mathcal{T}_h$, we have

$$h_T \leq \kappa h_E \tag{2.1}$$

We also introduce the shorthand notation for broken inner products over

\mathcal{T}_h and $\partial\mathcal{T}_h$ respectively as

$$(f, g)_{\mathcal{T}_h} := \sum_{T \in \mathcal{T}_h} (f, g)_T = \sum_{T \in \mathcal{T}_h} \int_T fg \, dx,$$

$$\langle f, g \rangle_{\partial\mathcal{T}_h} := \sum_{T \in \mathcal{T}_h} \langle f, g \rangle_{\partial T} = \sum_{T \in \mathcal{T}_h} \int_{\partial T} f g \, dx.$$

In the above, we have used the shorthand ∂T to denote the boundary of each cell $T \in \mathcal{T}_h$. The notation $\|\cdot\|_S$ denotes the L^2 norm over any S belonging to \mathcal{T}_h or \mathcal{E}_h . Here and in the sequel, we employ the standard notation for well-known Lebesgue and Sobolev spaces and norms defined on them (cf., e.g, [39, Section 1.2]). Throughout this paper, we use the symbol \lesssim to denote bounds involving positive constants independent of the local mesh size and ε .

2.1. Weak Differential Operators

Following [18], we introduce the definitions of the weak gradient and divergence operators. For any $T \in \mathcal{T}_h$, we let $V(T)$, denote the space of weak functions on T as

$$V(T) := \left\{ v = \{v_0, v_b\} : v_0 \in L^2(T), v_b \in H^{\frac{1}{2}}(\partial T), \right\}$$

and define the weak gradient as follows.

Definition 2.1 (Weak Gradient). *Given $v \in V(T)$,*

$$(\nabla_w v, \mathbf{q})_T := - \int_T v_0 \operatorname{div} \mathbf{q} \, dx + \int_{\partial T} v_b \mathbf{n} \cdot \mathbf{q} \, ds \quad \forall \mathbf{q} \in H(\operatorname{div}; T),$$

where \mathbf{n} is the outward unit normal vector to ∂T and

$$H(\operatorname{div}; T) := \{\mathbf{q} : \operatorname{div} \mathbf{q} \in L^2(T)\}.$$

On T , let $P_k(T)$ denote the space of all polynomials with degree no greater than k . For a given integer $k \geq 1$, let $V_{h,k}$ be the weak Galerkin finite element space corresponding to \mathcal{T}_h defined as follows:

$$V_{h,k} : \{v = \{v_0, v_b\} : v_0|_T \in P_k(T), v_b|_{\partial T} \in P_k(\partial T), T \in \mathcal{T}_h\},$$

and let V_h^0 be its subspace defined as:

$$V_{h,k}^0 : \{v = \{v_0, v_b\} \in V_{h,k} : v_b = 0, \text{ on } \partial\Omega\}.$$

We introduce the definition of the discrete weak gradient as described in [17].

Definition 2.2 (Discrete Weak Gradient). *For any $v = \{v_0, v_b\} \in V_{h,k}$ and for any $T \in \mathcal{T}_h$, the discrete weak gradient $\nabla_{w,k}v \in P_{k-1}(T)^2$ is defined on T as the unique polynomial satisfying*

$$(\nabla_{w,k}v, \boldsymbol{\psi})_T = -(v_0, \operatorname{div}\boldsymbol{\psi})_T + \langle v_b, \boldsymbol{\psi} \cdot \mathbf{n} \rangle_{\partial T} \quad \forall \boldsymbol{\psi} \in P_{k-1}(T)^2, \quad (2.2)$$

where \mathbf{n} is the outward unit normal to ∂T .

We note that since the right-hand side of (2.2) defines a bounded linear functional on $H(\operatorname{div}; T)$, the definition of discrete weak gradient (2.2) is well defined for $\boldsymbol{\psi} \in H(\operatorname{div}; T)$ as well. Thus,

$$\begin{aligned} (\nabla_{w,k}v, \boldsymbol{\psi})_T &= -(v_0, \operatorname{div}\boldsymbol{\psi})_T + \langle v_b, \boldsymbol{\psi} \cdot \mathbf{n} \rangle_{\partial T} \\ &= (\nabla_w v, \boldsymbol{\psi})_T, \quad \boldsymbol{\psi} \in H(\operatorname{div}; T). \end{aligned} \quad (2.3)$$

Next, we introduce the weak divergence operator by first defining the space of weak vector-valued functions on T as

$$\mathbf{V}(T) := \left\{ \{\mathbf{v}_0, \mathbf{v}_b\} : \mathbf{v}_0 \in L^2(T)^2, \mathbf{n} \cdot \mathbf{v}_b \in H^{-\frac{1}{2}}(\partial T) \right\},$$

so that the weak divergence operator can be defined as follows.

Definition 2.3 (Weak Divergence). *For $\mathbf{v} \in \mathbf{V}(T)$,*

$$(\nabla_w \cdot \mathbf{v}, \psi)_T := -(\mathbf{v}_0, \nabla\psi)_T + \langle \mathbf{v}_b \cdot \mathbf{n}, \psi \rangle_{\partial T} \quad \psi \in H^1(T)$$

where

$$H^1(T) := \{v : \nabla v \in L^2(T)\}.$$

Following [17], the discrete weak divergence is defined as follows.

Definition 2.4 (Discrete Weak Divergence). *Given $v = \{v_0, v_b\} \in V_{h,k}$ and for any $T \in \mathcal{T}_h$, a discrete weak divergence $\nabla_{w,k} \cdot (\mathbf{b}v) \in P_k(T)$ associated with \mathbf{b} can be defined as the unique polynomial satisfying*

$$(\nabla_{w,k} \cdot (\mathbf{b}v), \psi)_T = -(\mathbf{b}v_0, \nabla\psi)_T + \langle \mathbf{b} \cdot \mathbf{n}v_b, \psi \rangle_{\partial T} \quad \forall \psi \in P_k(T), \quad (2.4)$$

where \mathbf{n} is the outward unit normal to ∂T .

Notice that the above definition 2.4 holds true for $\boldsymbol{\psi} \in H^1(T)$. This is because the right-hand side of (2.4) defines a bounded linear functional on $H^1(T)$. Thus for $\psi \in H^1(T)$, we have

$$(\nabla_{w,k} \cdot (\mathbf{b}v), \psi)_T = -(\mathbf{b}v_0, \nabla\psi)_T + \langle \mathbf{b} \cdot \mathbf{n}v_b, \psi \rangle_{\partial T} = (\nabla_w \cdot (\mathbf{b}v), \psi)_T. \quad (2.5)$$

In view of (2.3) and (2.5), we drop the subscript “ k ” from the discrete weak differential operator $\nabla_{w,k}$ and instead adopt the notation ∇_w and $\nabla_w \cdot$ whenever the context is clear.

2.2. Weak Galerkin Method

For $w_h = \{w_{h0}, w_{hb}\}$ and $v_h = \{v_{h0}, v_{hb}\}$ in $V_{h,k}$, we define a bilinear form as

$$a_h(w_h, v_h) := \varepsilon(\nabla_w w_h, \nabla_w v_h)_{\mathcal{T}_h} + (aw_{h0} + \nabla_w \cdot (\mathbf{b}w_h), v_{h0})_{\mathcal{T}_h} + s(w_h, v_h), \quad (2.6)$$

where $s(w_h, v_h) = \langle \tau^+(w_{h0} - w_{hb}), v_{h0} - v_{hb} \rangle_{\partial\mathcal{T}_h}$ with τ^+ defining the stabilization parameter defined as:

$$\tau^+|_{\partial T} = (\mathbf{b} \cdot \mathbf{n}) \mathbf{I}_{\partial T^+} + \varepsilon(\kappa h_T)^{-1} + (\|\mathbf{b}\|_{\infty} \varepsilon^{-1} + 1)h_T + \varepsilon h_T^{-1}, \quad \forall T \in \mathcal{T}_h,$$

with the constant $\kappa > 0$ introduced in (2.1) and

$$I_{\partial T^+}(x) = \begin{cases} 1 & \text{if } \mathbf{b}(x) \cdot \mathbf{n}(x) \geq 0, \\ 0 & \text{otherwise.} \end{cases}$$

A weak Galerkin approximation for (1.1) amounts to seeking $u_h = \{u_{h0}, u_{hb}\} \in V_{h,k}^0$ satisfying the following equation:

$$a_h(u_h, v_h) = (f, v_{h0}) \quad \forall v_h = \{v_{h0}, v_{hb}\} \in V_h^0. \quad (2.7)$$

We equip the space V_h^0 with the following weak Galerkin energy norm

$$\|v_h\|^2 := \varepsilon \|\nabla_{w,k} v_h\|_{\mathcal{T}_h}^2 + \|v_0\|_{\mathcal{T}_h}^2 + \langle \tau(v_{h0} - v_{hb}), v_{h0} - v_{hb} \rangle_{\partial\mathcal{T}_h}. \quad (2.8)$$

where

$$\tau|_{\partial T} = |\mathbf{b} \cdot \mathbf{n}| + (\varepsilon h_T^{-1} + \varepsilon(\kappa h_T)^{-1} + \|\mathbf{b}\|_{\infty} \varepsilon^{-1} + 1)h_T \quad \forall T \in \partial\mathcal{T}_h.$$

The present work modifies the WG method of Lin and co-authors [17, eq. (2.8)] for solving the convection-diffusion equation with an additional diffusion-dependent stability term $\langle (\varepsilon \kappa h_T^{-1} + h_T)(w_{h0} - w_{hb}), v_{h0} - v_{hb} \rangle_{\partial\mathcal{T}_h}$. The presence of this additional stability term enables us to bound several terms of the a posteriori error estimator.

Associated with the solution u satisfying (1.1a)–(1.1b) and $u_h \in V_h$ satisfying (2.7), we introduce the following weak function measuring the error

$$e_h := \{e_{h0}, e_{hb}\} = \{u_0 - u_{h0}, u_b - u_{hb}\}, \quad (2.9)$$

where u_0 and u_b are understood to be the restrictions of u to the interior and the boundary of each $T \in \mathcal{T}_h$. Furthermore, following the discussion in [18, Section 3], for any $T \in \mathcal{T}_h$, an application of Green formula reveals

$$\begin{aligned} (\nabla u, \mathbf{q})_T &= -(u, \operatorname{div} \mathbf{q})_T + \langle u, \mathbf{n} \cdot \mathbf{q} \rangle_{\partial T} \\ &= -(u_0, \operatorname{div} \mathbf{q})_T + \langle u_b, \mathbf{n} \cdot \mathbf{q} \rangle_{\partial T} = (\nabla_w u, \mathbf{q})_T, \quad \mathbf{q} \in P_{m-1}(T)^2. \end{aligned}$$

This allows us to measure the error in the energy norm:

$$|||u - u_h|||^2 = \varepsilon \|\nabla_w u - \nabla_w u_h\|_{\mathcal{T}_h}^2 + \|\tau^{1/2}(u_{h0} - u_{hb})\|_{\partial \mathcal{T}_h}^2 + \|u - u_{h0}\|_{\mathcal{T}_h}^2 \quad (2.10)$$

where $\nabla_w u_h$ is understood to be the discrete weak gradient $\nabla_{w,k} u_h$ of $u_h \in V_{h,k}$ while $\nabla_w u$ is the classical derivative of u .

The well-posedness of the WG formulation is guaranteed thanks to the following Lemma which appeared in of [17, Section 3.1] and readily applies to our WG form.

Lemma 2.1 (Coercivity and Continuity). *There exists constants c_1 and c_2 such that there holds*

$$a_h(w, v) \leq c_1 |||w||| |||v||| \quad \forall w, v \in V_h, \quad (2.11)$$

$$c_2 |||v|||^2 \leq a_h(v, v), \quad \forall v \in V_h. \quad (2.12)$$

Proof. The proof has been provided in subsection 3.1 of [17]. \square

Remark 2.1. *While the above Lemma 2.1 guarantees the well-posedness of the WG method (2.7), the constant c_1 appearing in (2.11) have an undesirable dependence on ε^{-1} . This dependence arises when trying to control the term $(\nabla_w \cdot (\mathbf{b}u), w)$. Hence, our a posteriori error analysis cannot rely on the continuity property to control this term. Instead, inspired by the strategy in [13], we control this term by including the following semi-norm $|\cdot|_*$ to our energy norm (2.8).*

Definition 2.5 (Operator). *For any $\mathbf{q} \in L^2(\Omega)^2$, we define the following semi-norm $|\cdot|_*$ as*

$$|\mathbf{q}|_* = \sup_{w \in H_0^1(\Omega) \setminus \{0\}} \frac{\int_{\Omega} \mathbf{q} \cdot \nabla w \, dx}{|||w|||}. \quad (2.13)$$

The definition above is well defined because \mathbf{q} admits the following Helmholtz decomposition

$$\mathbf{q} = \nabla\phi + \mathbf{q}_0, \quad (2.14)$$

where $\phi \in H_0^1(\Omega)$ uniquely solves

$$\int_{\Omega} \nabla\phi \cdot \nabla w \, dx = \int_{\Omega} \mathbf{q} \cdot \nabla w \, dx \quad \forall w \in H_0^1(\Omega),$$

and $\mathbf{q}_0 = \mathbf{q} - \nabla\phi$ satisfies the divergence-free property

$$\int_{\Omega} \mathbf{q}_0 \cdot \nabla w \, dx = 0 \quad \forall w \in H_0^1(\Omega).$$

The decomposition (2.14) is unique and orthogonal in $L^2(\Omega)^2$.

Consequently, we have the following upper bound:

For $u_h = \{u_{h0}, u_{hb}\} \in V_{h,k}$, $v \in H_0^1(\Omega)$,

$$(\nabla_w \cdot (\mathbf{b}u_h), v) \leq |\mathbf{b}u_{h0}|_* |||v|||, \quad (2.15)$$

where $|||v|||^2 := \varepsilon \|\nabla v\|^2 + \|v\|^2$. Inequality (2.15) holds because

$$(\nabla_w \cdot (\mathbf{b}u_h), v)_{\mathcal{T}_h} = -(\mathbf{b}u_{h0}, \nabla v)_{\mathcal{T}_h} + \langle \mathbf{n} \cdot \mathbf{b}u_{hb}, v \rangle_{\partial\mathcal{T}_h}$$

and using the fact that $\langle \mathbf{n} \cdot \mathbf{b}u_{hb}, v \rangle_{\partial\mathcal{T}_h} = 0$.

Remark 2.2 (Practical estimation of $|\mathbf{b}(u - u_{h0})|_*$). Following the arguments presented in [13, Remark 3.5], we use the following inequality

$$|(u - u_{h0})|_* \lesssim \frac{1}{\sqrt{\varepsilon}} \|u - u_{h0}\|$$

to serve as a computable upper bound for $|\mathbf{b}(u - u_{h0})|_*$.

We close this section by proving the inf-sup condition for $a_h(\cdot, \cdot)$ on $H_0^1(\Omega)$. The proof follows the arguments presented in [13]. However, since our definition of the energy norm $|||u||| + |\mathbf{b}u|_*$ differs from the one used in [13], we include the proof below for completeness.

Theorem 2.1 (inf-sup condition). *There exists a constant $C > 0$ satisfying*

$$\inf_{u \in H_0^1(\Omega) \setminus \{0\}} \sup_{v \in H_0^1(\Omega) \setminus \{0\}} \frac{a_h(u, v)}{(\|u\| + |\mathbf{b}u|_*) \|v\|} \geq C > 0. \quad (2.16)$$

Proof. Let $u \in H_0^1(\Omega)$ and $0 < \theta < 1$. There exists $w_\theta \in H_0^1(\Omega)$ such that

$$\|w_\theta\| = 1, \quad (\nabla_w \cdot (\mathbf{b}u), w_\theta) \geq \theta |\mathbf{b}u|_*.$$

$$\begin{aligned} (\varepsilon \nabla u, -\nabla w_\theta) + (au, -w_\theta) &\leq \|\varepsilon^{1/2} \nabla u\| \|\varepsilon^{1/2} \nabla w_\theta\| + \|a\|_\infty \|u\| \|w_\theta\| \\ &\leq \max\{1, \|a\|_\infty\} \|u\|. \end{aligned}$$

Thus,

$$\begin{aligned} a_h(u, w_\theta) &= (\varepsilon \nabla u, \nabla w_\theta) + (au, w_\theta) + (\nabla_w \cdot (\mathbf{b}u), w_\theta) \\ &\geq -c_1 \|u\| + \theta |\mathbf{b}u|_*, \end{aligned} \quad (2.17)$$

where $c_1 = \max\{1, \|a\|_\infty\}$. Noting that

Next, we define $v_\theta = u + \alpha w_\theta$ where $\alpha > 0$ is chosen suitably. Using

$$\begin{aligned} a_h(u, u) &\geq \varepsilon \|\nabla_w u\|^2 + (c_0 u, u) \\ &\geq c_* \|u\|^2 \quad \text{where } c_* = \min\{1, c_0\} \end{aligned} \quad (2.18)$$

and (2.17), we have

$$\begin{aligned} a_h(u, v_\theta) &= a_h(u, u) + \alpha a_h(u, w_\theta) \\ &\geq c_* \|u\|^2 + \alpha (-c_1 \|u\| + \theta |\mathbf{b}u|_*). \end{aligned} \quad (2.19)$$

We pick $\alpha = c_* \|u\| / (c_1 + 1)$ so that,

$$\begin{aligned} a_h(u, v_\theta) &\geq (c_1 + 1)^{-1} c_* (\|u\| + \theta |\mathbf{b}u|_*) \|u\| \quad \text{and,} \\ \|v_\theta\| &= (c_1 + 1)^{-1} \{c_1 + 1 + c_*\} \|u\| \\ \text{thus, } \frac{a_h(u, v_\theta)}{\|v_\theta\|} &\geq \frac{c_* (\|u\| + \theta |\mathbf{b}u|_*)}{\{c_1 + 1 + c_*\}} = C (\|u\| + \theta |\mathbf{b}u|_*) \end{aligned}$$

where $C = c_* \{c_1 + 1 + c_*\}^{-1} > 0$.

Consequently, for any $u \in H_0^1(\Omega)$, $\theta \in (0, 1)$, we have

$$C (\|u\| + \theta |\mathbf{b}u|_*) \leq \frac{a_h(u, v_\theta)}{\|v_\theta\|} \leq \sup_{v \in H_0^1(\Omega)} \frac{a_h(u, v)}{(\|u\| + |\mathbf{b}u|_*) \|v\|}$$

from which, the result follows. \square

3. A Posteriori Error Analysis

In this section, we present a residual-based estimator and prove its reliability and efficiency.

Definition 3.1 (Estimator). *We introduce the estimator in terms of the cell and edge indicators defined as shown below:*

$$\eta_h^2 := \sum_{T \in \mathcal{T}_h} \left(\eta_{T,1}^2 + \eta_{T,2}^2 \right) + \sum_{E \in \mathcal{E}_h} \eta_E^2, \quad (3.1)$$

where the cell and edge residuals are

$$\begin{aligned} \eta_{T,1}^2 &:= \alpha_T^2 \|R_h\|_T^2, \quad \text{with } R_h := f_h + \operatorname{div}(\varepsilon \nabla_w u_h) - \nabla_w \cdot (\mathbf{b} u_{h0}) - a_h u_{h0}, \\ \eta_{T,2}^2 &:= \langle \tau(u_{h0} - u_{hb}), u_{h0} - u_{hb} \rangle_{\partial T}, \\ \eta_E^2 &:= \alpha_E \varepsilon^{-1/2} \|J_h\|_E^2, \quad \text{with } J_h := [\varepsilon \mathbf{n} \cdot \nabla_w u_h], \end{aligned} \quad (3.2)$$

and the weights are according to [20, equation (3.4)]

$$\alpha_T = \min\{h_T \varepsilon^{-1/2}, c_0^{-1/2}\}, \quad \text{and} \quad \alpha_E = \min\{h_E \varepsilon^{-1/2}, c_0^{-1/2}\}. \quad (3.3)$$

We note that if $c_0 = 0$, we define the weights as follows

$$\alpha_T = \min\{h_T \varepsilon^{-1/2}, 1\}, \quad \text{and} \quad \alpha_E = \min\{h_E \varepsilon^{-1/2}, 1\}. \quad (3.4)$$

We also define the oscillation of data as

$$\operatorname{osc}(f, a) = \left(\sum_{T \in \mathcal{T}_h} \alpha_T^2 (\|f - f_h\|_T^2 + \|(a - a_h)u_{h0}\|_T^2) \right)^{1/2}. \quad (3.5)$$

3.0.1. Reliability of Estimator

This subsection is devoted to proving the reliability for the estimator defined in (3.1). The proof of the reliability relies on decomposing the discretization error into its conforming and non-conforming component and deriving upper bounds for each component. To this end, we first introduce a suitable conforming discrete space $V_h^c = V_h \cap H_0^1(\Omega)$.

For any $v_h = \{v_{h0}, v_{hb}\} \in V_h$ we associate a conforming approximation $v_{h0}^c \in V_h^c$. Construction of such an approximation is a standard DG tool in the error analysis (see [40, Theorems 2.2 and 2.3] for instance). This allows us to decompose v_h as

$$v_h = v_h^c + v_h^r \quad (3.6)$$

where the nonconforming component $v_h^r = \{v_{h0} - v_h^c, v_{hb} - v_h^c\} \in V_h$. The above conforming approximation satisfies the following properties:

$$\|v_{h0} - v_h^c\|_{\mathcal{T}_h}^2 \lesssim \sum_{E \in \mathcal{E}_h} \int_E h_E [v_{h0}]^2 ds, \quad (3.7a)$$

$$\|\nabla v_{h0} - \nabla v_h^c\|_{\mathcal{T}_h}^2 \lesssim \sum_{E \in \mathcal{E}_h} \int_E h_E^{-1} [v_{h0}]^2 ds. \quad (3.7b)$$

Thanks to the single-valuedness of v_{hb} over each edge $E \in \mathcal{E}_h$, the jump term in the rhs of (3.9) and (3.10) can be expressed as

$$\begin{aligned} \sum_{E \in \mathcal{E}_h} \int_E [v_{h0}]^2 ds &= \sum_{E \in \mathcal{E}_h} \int_E [v_{h0} - v_{hb}]^2 ds \\ &\leq \sum_{T \in \mathcal{T}_h} \int_{\partial T} 2(v_{h0} - v_{hb})^2 ds. \end{aligned} \quad (3.8)$$

Using (3.8) in (3.7) and by using $\kappa h_T \leq h_E$, and $h_E \leq h_T$, we have

$$\|v_{h0} - v_h^c\|_{\mathcal{T}_h}^2 \lesssim \sum_{T \in \mathcal{T}_h} h_T \int_{\partial T} (v_{h0} - v_{hb})^2 ds, \quad (3.9)$$

$$\|\nabla v_{h0} - \nabla v_h^c\|_{\mathcal{T}_h}^2 \lesssim \sum_{T \in \mathcal{T}_h} (\kappa h_T)^{-1} \int_{\partial T} (v_{h0} - v_{hb})^2 ds. \quad (3.10)$$

The lemma below provides bounds for the non-conforming component.

Lemma 3.1 (Nonconforming term bound). *For $v_h \in V_h$ admitting the decomposition (3.6) the following hold true:*

$$a_h(v_h^r, w) \lesssim \max\{1, \|a\|_\infty, \|\mathbf{b}\|_\infty\} \|v_h^r\| \|w\|, \quad w \in H_0^1(\Omega), \quad (3.11)$$

$$\|v_h^r\| + |\mathbf{b}v_{h0}^r|_* \lesssim \sum_{T \in \mathcal{T}_h} (\varepsilon h_T^{-1} + \varepsilon(\kappa h_T)^{-1} + h_T) \|v_{h0} - v_{hb}\|_{\partial T}^2. \quad (3.12)$$

Proof. To see (3.11), we apply the definitions of the WG form and weak divergence

$$\begin{aligned} a_h(v_h^r, w) &= (\varepsilon \nabla_w v_h^r, \nabla w)_{\mathcal{T}_h} - (\mathbf{b}v_{h0}^r, \nabla w)_{\mathcal{T}_h} + (av_{h0}^r, w)_{\mathcal{T}_h} + \langle \mathbf{n} \cdot \mathbf{b}v_{hb}^r, w \rangle_{\partial \mathcal{T}_h} \\ &\leq \left(\|v_h^r\| + \|\mathbf{b}\|_\infty \varepsilon^{-1/2} \|v_{h0}^r\| + \|a\|_\infty \|v_{h0}^r\| \right) \|w\|, \\ &\leq \max\{1, \|a\|_\infty, \|\mathbf{b}\|_\infty\} \|v_h^r\| \|w\|, \quad w \in H_0^1(\Omega). \end{aligned}$$

Here we have used (3.9) and $\langle \mathbf{n} \cdot \mathbf{b}u_{hb}^r, w \rangle_{\partial \mathcal{T}_h} = 0$.

Next, for deriving (3.12), we use the definition (2.2) of the weak gradient in conjunction with the trace, inverse and Cauchy-Schwarz inequalities and (3.9) to obtain

$$\begin{aligned} \|\nabla_w v_h^r\|_T^2 &= (\nabla v_{h0}^r, \nabla_w v_h^r)_T - \langle v_{h0}^r - v_b^r, \mathbf{n} \cdot \nabla_w v_h^r \rangle_{\partial T} \\ &\leq \left(\|\nabla v_{h0}^r\|_T + Ch_T^{-1/2} \|v_{h0}^r - v_{hb}^r\|_{\partial T} \right) \|\nabla_w v_h^r\|_T \\ \varepsilon^{1/2} \|\nabla_w v_h^r\|_T &\leq \min\{1, C\} \left(\varepsilon \|\nabla v_{h0}^r\|_T^2 + \varepsilon h_T^{-1} \|v_{h0} - v_{hb}\|_{\partial T}^2 \right)^{1/2} \end{aligned}$$

Thus, summing over all $T \in \mathcal{T}_h$,

$$\varepsilon \|\nabla_w v_h^r\|_{\mathcal{T}_h}^2 \lesssim \sum_{E \in \mathcal{E}_h} \int_E \varepsilon h_E^{-1} [v_{h0}]^2 ds + \sum_{T \in \mathcal{T}_h} \varepsilon h_T^{-1} \|v_{h0} - v_{hb}\|_{\partial T}^2. \quad (3.13)$$

Using (3.8) in (3.13) and (3.9) we obtain

$$\varepsilon \|\nabla_w v_h^r\|_{\mathcal{T}_h}^2 + \|v_{h0}^r\|_{\mathcal{T}_h}^2 \lesssim \sum_{T \in \mathcal{T}_h} (\varepsilon h_T^{-1} + \varepsilon (\kappa h_T)^{-1} + h_T) \|v_{h0} - v_{hb}\|_{\partial T}^2. \quad (3.14)$$

Finally, for bounding $|\mathbf{b}v_{h0}^r|_*$, we use (3.9), Cauchy-Schwarz inequality and the definition of $|\mathbf{b}v_{h0}^r|_*$

$$\begin{aligned} |\mathbf{b}v_{h0}^r|_* &\lesssim \varepsilon^{-1/2} \|\mathbf{b}\|_\infty \|v_{h0}^r\|_{\mathcal{T}_h} \\ &\lesssim \|\mathbf{b}\|_\infty \left(\sum_{T \in \mathcal{T}_h} \varepsilon^{-1} h_T \|v_{h0} - v_{hb}\|_{\partial T}^2 \right)^{1/2}. \end{aligned} \quad (3.15)$$

□

Next, we proceed to control the conforming term by first deriving the error equation. To this end, we introduce the following continuous subspace

$$V_{h,1}^c := \{w \in H_0^1(\Omega) : w|_K \in P_1(T), T \in \mathcal{T}_h\}$$

and observe that by setting v_b as trace of v on all the edges $E \in \partial \mathcal{T}_h$, $V_{h,1}^c$ can be naturally embedded in V_h . This approach was used within the adaptive WG framework by Chen et al. [34] for obtaining partial orthogonality for second order elliptic problems.

We also introduce the following Clément interpolation operator specially designed for convection diffusion problems by Verfürth [20, Lemma 3.3] and

references therein. We denote this operator by $\Pi_h : H_0^1 \rightarrow V_{h,1}^c$ satisfying $|||\Pi_h v||| \lesssim |||v|||$ and

$$\left(\sum_{T \in \mathcal{T}_h} \alpha_T^{-2} \|v - \Pi_h v\|_T^2 \right)^{1/2} \lesssim |||v|||, \quad (3.16)$$

$$\left(\sum_{E \in \mathcal{E}_h} \varepsilon^{1/2} \alpha_E^{-1} \|v - \Pi_h v\|_E^2 \right)^{1/2} \lesssim |||v|||, \quad v \in H_0^1(\Omega). \quad (3.17)$$

It is easy to see that for u satisfying (1.1) and $u_h \in V_h$ satisfying the WG form (2.7), the following holds true:

$$a_h(u - u_h, v_h^c) = 0 \quad \forall v_h^c \in V_{h,1}^c. \quad (3.18)$$

As a consequence, we have the following error equation.

Lemma 3.2 (Error Equation). *Let u solve (1.1a)–(1.1b), $u_h \in V_h$ solve (2.7) decomposed as $u_h = u_h^c + u_h^r$ according to the decomposition (3.6). Then, for any $v \in H_0^1(\Omega)$,*

$$a_h(u - u_h, v) = (\text{osc}(f, a), \hat{v}) + (R_h, \hat{v}) - \langle J_h, \hat{v} \rangle \quad (3.19)$$

where $\hat{v} = v - \Pi_h^c v$ and $\text{osc}(f, a)$, R_h and J_h are defined in (3.5) (3.2) respectively.

Proof. Since the exact solution u solves (1.1a)–(1.1b), we obtain, by applying (3.18) for $\Pi_h^c v \in V_{h,1}^c$,

$$\begin{aligned} a_h(u - u_h, v) &= (f, v) - a_h(u_h, v) \\ &= (f, v - \Pi_h^c v) - a_h(u_h, v - \Pi_h^c v) + \{(f, \Pi_h^c v) - a_h(u_h, \Pi_h^c v)\} \\ &= (f - f_h + a_h u_{h0} - a u_{h0}, \hat{v}) + (R_h, \hat{v}) - \langle J_h, \hat{v} \rangle. \end{aligned} \quad (3.20)$$

To obtain (3.20), we have added and subtracted the data $(f_h - a_h u_{h0}, \hat{v})$ and for the last two terms of (3.20) we apply integration by parts to $\varepsilon(\nabla_w u_h, \nabla_w \hat{v})$. \square

Lemma 3.3 (Conforming term bound). *Let u solve (1.1a)–(1.1b) and $u_h \in V_h$ solve (2.7) and express $u_h = u_h^c + u_h^r$ according to (3.6). For any $v \neq 0 \in H_0^1(\Omega)$,*

$$|||u - u_h^c||| + |\mathbf{b}(u - u_h^c)|_* \lesssim \frac{a_h(u_h^r, v)}{|||v|||} + \eta_h + \text{osc}(f, a). \quad (3.21)$$

Proof. Thanks to the inf-sup condition (2.16), for any $v \in H_0^1(\Omega) \setminus \{0\}$,

$$|||u - u_h^c||| + |\mathbf{b}(u - u_h^c)|_* \lesssim \frac{a_h(u - u_h^c, v)}{|||v|||}. \quad (3.22)$$

Now, for the rhs of (3.22), using $u_h^c = u_h - u_h^r$ and (3.19) we have

$$\begin{aligned} a_h(u - u_h^c, v) &= (f, v) - a_h(u_h - u_h^r, v) \\ &= a_h(u_h^r, v) + (f, v) - a_h(u_h, v) \\ &= a_h(u_h^r, v) + (\text{osc}(f, a), \hat{v}) + (R_h, \hat{v}) - \langle J_h, \hat{v} \rangle. \end{aligned} \quad (3.23)$$

In view of (3.23) and (3.22) and using the approximation properties (3.16) and (3.16) we obtain the desired upper bound. \square

We are now in the position to prove the reliability of the estimator.

Theorem 3.1 (Reliability). *Let u solve (1.1) and $u_h \in V_h$ be the WG approximation to (2.7). Then,*

$$|||u - u_h||| + |\mathbf{b}(u - u_{h0})|_* \lesssim \eta_h + \text{osc}(f, a). \quad (3.24)$$

Proof. Decompose $u_h = u_h^c + u_h^r$ where $u_h^c \in V_h^c$. By the triangle inequality and Lemma 3.3, for any nonzero $v \in H_0^1(\Omega)$,

$$\begin{aligned} |||u - u_h||| + |\mathbf{b}(u - u_{h0})|_* &\leq |||u - u_h^c||| + |\mathbf{b}(u - u_h^c)|_* + |||u_h^r||| + |\mathbf{b}u_{h0}^r|_* \\ &\lesssim \frac{a_h(u_h^r, v)}{|||v|||} + \eta_h + \text{osc}(f, a) + |||u_h^r||| + |\mathbf{b}u_{h0}^r|_* \end{aligned}$$

The result now follows thanks to Lemma 3.1. \square

Theorem 3.2 (Efficiency).

$$\eta_h \lesssim |||u - u_h||| + |\mathbf{b}(u - u_{h0})|_* + \text{osc}(f, a). \quad (3.25)$$

Proof. Efficiency will be shown through the following lemmas which employ the bubble function techniques introduced by Verfürth[20]. We remark that the arguments presented here are simpler than its DG counterpart presented in [13] thanks to the simpler weak form. \square

Lemma 3.4 (Cell efficiency).

$$\left(\sum_{T \in \mathcal{T}_h} (\eta_{T,1}^2 + \eta_{T,2}^2) \right)^{1/2} \lesssim |||u - u_h||| + |\mathbf{b}(u - u_{h0})|_* + \text{osc}(f, \mathbf{b}, a). \quad (3.26)$$

Proof. It is easy to see that $\sum_{T \in \mathcal{T}_h} \eta_{T,2}^2 \leq |||u - u_h|||^2$. Now for bounding $\sum_{T \in \mathcal{T}_h} \eta_{T,1}^2$, we let b_T denote the element-bubble function described in [20, p. 1771] for any cell $T \in \mathcal{T}_h$. We first take

$$v_T = \alpha_T^2 R_h b_T.$$

Since R_h belongs to a finite dimensional space on T , a local equivalence of norms yields

$$\int_T \alpha_T^2 |R_h|^2 dx \lesssim \int_T \alpha_T^2 R_h^2 b_T dx = \int_T R_h v_T dx. \quad (3.27)$$

Since the exact solution u satisfies the strong form $-\varepsilon \operatorname{div} \nabla u + \operatorname{div}(\mathbf{b}u) + au = f$ on each $T \in \mathcal{T}_h$, by adding and subtracting the exact data and applying integration by parts to $\int_T \operatorname{div}(\varepsilon \nabla_w u - \varepsilon \nabla_w u_h) v_T dx$ in conjunction with $v_T|_{\partial T} = 0$, we have

$$\begin{aligned} \int_T R_h v_T dx &= \int_T \varepsilon (\nabla_w u - \nabla_w u_h) \cdot \nabla_w v_T dx + \\ &\int_T (\nabla_w \cdot (\mathbf{b}u) - \nabla_w \cdot (\mathbf{b}u_h) + a(u - u_{h0})) \nabla v_T dx + \\ &\int_T (f_h - f + (a_h - a)u_{h0}) v_T dx. \end{aligned} \quad (3.28)$$

Now combining (3.27) and (3.28), summing over all $T \in \mathcal{T}_h$ and applying Cauchy Schwarz inequality we obtain

$$\sum_{T \in \mathcal{T}_h} \eta_{T,1}^2 \lesssim (|||e_h||| + |\mathbf{b}e_h|_* + \operatorname{osc}(f, a)) \left(\sum_{T \in \mathcal{T}_h} |||v_T|||^2 + \alpha_T^{-2} \|v_T\|_T^2 \right)^{1/2}. \quad (3.29)$$

Thus,

$$\begin{aligned} \sum_{T \in \mathcal{T}_h} \eta_{T,1}^2 &\lesssim \left(|||e_h||| + |\mathbf{b}e_h|_* + \operatorname{osc}(f, a) \right) \\ &\left(|||v_T|||^2 + \sum_{T \in \mathcal{T}_h} \alpha_T^{-2} \|v_T\|_T^2 \right)^{1/2}. \end{aligned} \quad (3.30)$$

Using the following property of the element bubble function

$$|||\sigma b_T||| \lesssim \alpha_T^{-1} \|\sigma\|_{L^2(T)}, \quad \|b_T\|_\infty = 1$$

$|||v_T|||^2 \lesssim \alpha_T^2 \|R_h\|_{L^2(T)}$ and $\alpha_T^{-2} \|v_T\|_T^2 \lesssim \alpha_T^2 \|R_h\|_{L^2(T)}$ the assertion follows. \square

Lemma 3.5 (edge efficiency).

$$\left(\sum_{E \in \mathcal{E}_h} \eta_E^2 \right)^{1/2} \lesssim |||u - u_h||| + |\mathbf{b}(u - u_{h0})|_* + \text{osc}(f). \quad (3.31)$$

Proof. For any edge $E \in \mathcal{E}_h$, let b_E denote the edge-bubble function described in [20, p. 1771]. We first take

$$v_E = \varepsilon^{-1/2} \alpha_E J_h b_E.$$

Since R_h belongs to a finite dimensional space on T , once again we rely on a local equivalence of norms to obtain

$$\int_E J_h v_E ds \lesssim \int_E [\varepsilon \mathbf{n} \cdot \nabla_w u_h] v_E ds = - \int_E [\varepsilon \mathbf{n} \cdot \nabla_w e_h] v_E ds. \quad (3.32)$$

Let $\omega_E \subset \mathcal{T}_h$ denote the compact support of E and v_{ω_E} denote the extension of edge bubble function to ω_E .

$$\begin{aligned} & - \int_E [\varepsilon \mathbf{n} \cdot \nabla_w e_h] v_E ds = - \int_{\omega_E} \text{div} \varepsilon (\nabla_w u - \nabla_w u_h) v_{\omega_E} dx \\ & - \int_{\omega_E} \varepsilon (\nabla_w u - \nabla_w u_h) \cdot \nabla v_{\omega_E} dx \\ & \pm \int_{\omega_E} (\nabla_w \cdot (\mathbf{b}u) - \nabla_w \cdot (\mathbf{b}u_h) + au - a_h u_{h0}) \nabla v_{\omega_E} dx. \\ & = \int_{\omega_E} \text{osc}(f, a) v_{\omega_E} dx - \int_{\omega_E} (\nabla_w \cdot (\mathbf{b}e_h) + a e_{h0}) v_{\omega_E} dx \\ & + \int_{\omega_E} R_h v_{\omega_E} dx - \int_{\omega_E} \varepsilon \nabla_w e_h \cdot \nabla v_{\omega_E} dx \\ & \leq (\text{osc}(f, a) + |\mathbf{b}e_{h0}|_* + \|a\|_\infty \|e_{h0}\|) \|v_{\omega_E}\|_{\omega_E} + \sum_{T \in \omega_E} \alpha_T \eta_{T,1} \alpha_T^{-1} \|v_{\omega_E}\|_T \\ & + \|\varepsilon^{1/2} \nabla_w e_h\|_{\omega_E} \|\varepsilon^{1/2} \nabla v_{\omega_E}\|_{\omega_E} \end{aligned} \quad (3.33)$$

Using the properties of the edge bubble function

$$\|\sigma b_E\|_{\omega_E}^2 \lesssim \varepsilon^{1/4} \alpha_E^{1/2} \|\sigma\|_E^2,$$

and

$$|||\sigma b_E|||_{\omega_E}^2 \lesssim \varepsilon^{1/4} \alpha_E^{-1/2} \|\sigma\|_E^2,$$

the assertion follows. \square

4. Numerical Results

In this section we present the results of the following benchmark problems to test the performance of the estimator. The numerical implementation has been realized by using the C++ software library deal.II [41, 42]. Our sequence of adaptively refined rectangular meshes is constructed by selecting those elements for refinement which possess the top 25% of the largest local indicators η_T . Since we are using rectangular meshes, local grid refinement inevitably leads to irregular meshes, i.e., not every edge of a cell is also a complete edge of its neighboring cell. Consistent with our implementation, we restrict this irregularity to one-irregular meshes, that is, any edge of a cell is shared by at most two cells on the other side of the edge.

All the experiments were performed on the unit square $\Omega = (0, 1)^2$ with the initial grid consisting of 16×16 elements, using polynomial degree $k = 2, 3$. We remark that these examples have been previously investigated in [8, 16].

Since the norm used in proving the reliability and efficiency of the estimator involves the energy norm (2.8) and the unusual norm $|\mathbf{b}(u - u_{h0})|_*$, for the numerical experiments, we calculate $|\mathbf{b}(u - u_{h0})|_*$, by using the upper bound $\varepsilon^{-1/2}\|u - u_{h0}\|$ which has been described in [13, Remark 3.5].

4.1. Boundary Layer Benchmark

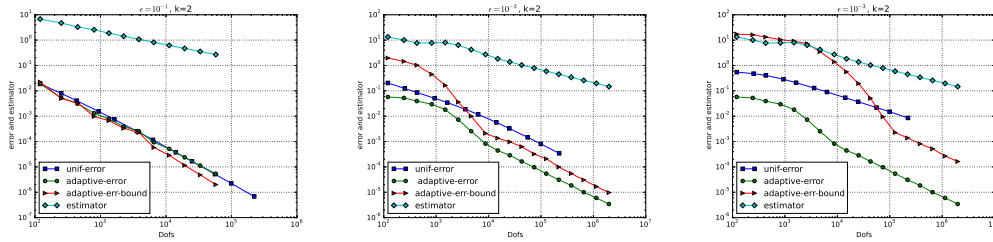


Figure 1: Boundary Layer Benchmark: Convergence history for $\varepsilon = 10^{-1}, 10^{-2}, 10^{-3}$ and $k = 2$.

We take $\mathbf{b} = (1, 1)^T$ and $a = 0$ with the diffusive coefficient varying between 10^{-3} to 10^{-1} . We pick the boundary conditions and the right-hand side $f(x, y)$ so that the analytical solution to (1.1) is

$$u(x, y) = x + y(1 - x) + \frac{e^{-\varepsilon^{-1}} - e^{-(1-x)(1-y)\varepsilon^{-1}}}{1 - e^{-\varepsilon^{-1}}}.$$

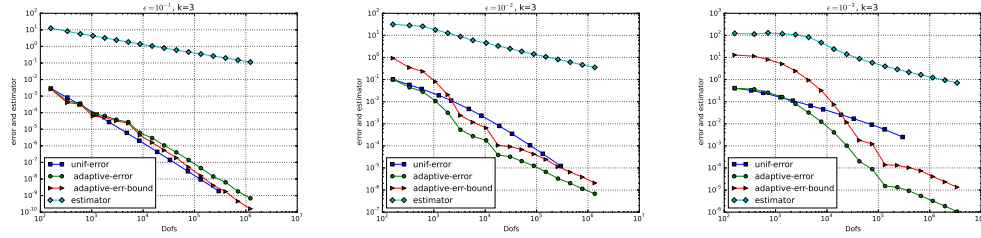


Figure 2: Boundary Layer Benchmark: Convergence history for $\varepsilon = 10^{-1}$, 10^{-2} , 10^{-3} and $k = 3$.

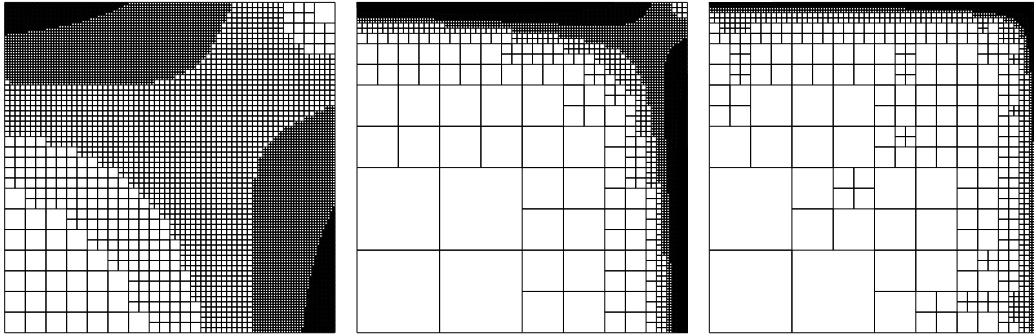


Figure 3: Boundary Layer Benchmark: Refined meshes after 11 levels of refinement for $\varepsilon = 10^{-1}$, (left) 10^{-2} , (center) 10^{-3} (right) and $k = 3$.

It is well known that when ε is small, the solution develops boundary layers at $x = 1$ and $y = 1$. These layers have width $\mathcal{O}(\varepsilon)$. In Figures 1 and 2, we demonstrate the performance of our estimator for $\varepsilon = 10^{-1}$, 10^{-2} , 10^{-3} using $k = 2$ and $k = 3$ respectively against the total degrees of freedom. In the same figures, we also plot the “true” energy error $\|u - u_h\|$ on adaptively refined meshes denoted by the curve “adaptive-error” and the curve “adaptive-err-bound”. The latter serves as a computable upper bound for $|\mathbf{be}_{ho}|_*$ (see Remark 2.2). We compare the performance of “adaptive-error” curve with the “true” energy error computed on uniformly refined meshes depicted by the curve “unif-error” plotted in the same figures.

As expected the estimator always overestimates the “true” energy norm thereby confirming the reliability of the estimator. Furthermore, after the boundary layers are sufficiently resolved for each choice of ε , the asymptotic regime is achieved. We remark that through the adaptive mesh refinement, we can achieve the expected convergence rates particularly for the interme-

diante regime $\varepsilon = 10^{-3}$, where the poor numerical behavior was observed on uniformly refined meshes. See [17, Example 2] and [8, Example 2]. This phenomena is numerically verified in Figures 1 and 2 for the uniform error curves. We notice that for $\varepsilon = 10^{-1}$, the adaptive error and uniform error curves are almost indistinguishable for $k = 2$ and certainly the uniform error curve outperforms the adaptive error curve for $k = 3$. The reason for this observation is that for $\varepsilon = 10^{-1}$, it takes only a few levels of uniform refinement for the mesh size to be fine enough to resolve the layer of width 10^{-1} .

In Figure 3, we present the adaptively refined meshes after 11 levels of refinement for $k = 3$. We notice a pronounced refinement along the lines $x = 1$ and $y = 1$ which suggests that our estimator accurately detects the boundary layers and is able to resolve them. We also notice that for $\varepsilon = 10^{-1}$, the width of the layer is “large” enough to be resolved within just a few levels of refinement.

4.2. Internal Layer Benchmark

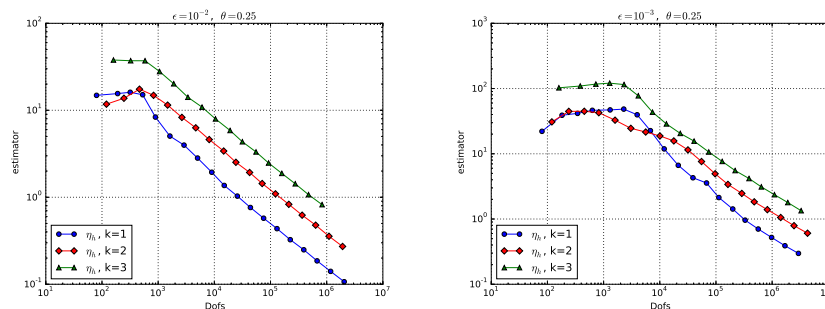


Figure 4: Internal Layer Benchmark: Convergence behavior for $\varepsilon = 10^{-2}$, (left) $\varepsilon = 10^{-3}$ (right) using $k = 3$.

In this example, we present the performance of the estimator in the presence of internal layers. We choose $\mathbf{b} = (\frac{1}{2}, \frac{\sqrt{3}}{2})$, $a = 0$, $f(x, y) = 0$ and the Dirichlet boundary conditions are chosen as:

$$u(x, y) = \begin{cases} 1 & \text{on } [0, 1] \times \{0\}, \\ 1 & \text{on } \{0\} \times [0, \frac{1}{5}], \\ 0 & \text{otherwise.} \end{cases}$$

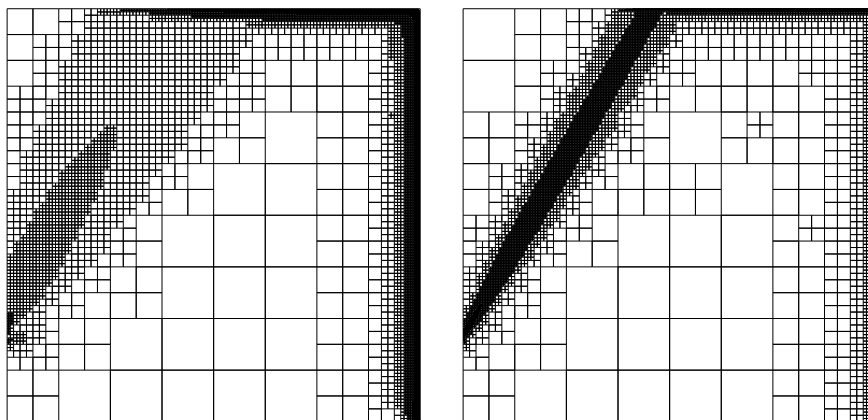


Figure 5: Internal Layer Benchmark: Adaptively refined after 11 levels of refinement for $\varepsilon = 10^{-2}$ (*left*) and $\varepsilon = 10^{-3}$ (*right*) using $k = 3$.

Since the boundary data is discontinuous at the inflow boundary, an internal layer occurs across the domain. In the absence of the exact solution to this problem, we present the convergence of the estimator for the cases $\varepsilon = 10^{-2}$ and $\varepsilon = 10^{-3}$ in Figure 4. In Figure 5, we present the meshes which are adaptively refined after 11 levels of refinement for the same values of ε . As expected, we observe the strong refinement concentrated along the internal layer as shown in demonstrating the performance of the estimator in successfully detecting the internal layer.

Acknowledgment

The author would like to thank Sara Pollock for her valuable advice and fruitful discussions related to the weak Galerkin method.

References

References

- [1] A. N. Brooks, T. J. Hughes, Streamline upwind/Petrov-Galerkin formulations for convection dominated flows with particular emphasis on the incompressible Navier-Stokes equations, *Computer Methods in Applied Mechanics and Engineering* 32 (1-3) (1982) 199–259.

- [2] T. J. Hughes, Finite element methods for convection dominated flows; Proceedings of the Winter Annual Meeting, New York, NY, December 2-7, 1979, Finite Element Methods for Convection Dominated Flows.
- [3] F. Brezzi, T. J. Hughes, L. Marini, A. Russo, E. Süli, A priori error analysis of residual-free bubbles for advection-diffusion problems, *SIAM Journal on Numerical Analysis* 36 (6) (1999) 1933–1948.
- [4] F. Brezzi, D. Marini, E. Süli, Residual-free bubbles for advection-diffusion problems: the general error analysis, *Numerische Mathematik* 85 (1) (2000) 31–47.
- [5] E. Burman, A. Ern, Stabilized Galerkin approximation of convection-diffusion-reaction equations: discrete maximum principle and convergence, *Mathematics of computation* 74 (252) (2005) 1637–1652.
- [6] B. Cockburn, C. Dawson, Some extensions of the local discontinuous Galerkin method for convection-diffusion equations in multidimensions.
- [7] P. Houston, C. Schwab, E. Süli, Discontinuous hp-finite element methods for advection-diffusion-reaction problems, *SIAM Journal on Numerical Analysis* 39 (6) (2002) 2133–2163.
- [8] B. Ayuso, L. D. Marini, Discontinuous galerkin methods for advection-diffusion-reaction problems, *SIAM Journal on Numerical Analysis* 47 (2) (2009) 1391–1420.
- [9] B. Cockburn, Discontinuous Galerkin methods for convection-dominated problems, in: *High-order methods for Computational Physics*, Springer, 1999, pp. 69–224.
- [10] H. Zarin, H.-G. Roos, Interior penalty discontinuous approximations of convection–diffusion problems with parabolic layers, *Numerische Mathematik* 100 (4) (2005) 735–759.
- [11] R. Becker, P. Hansbo, Discontinuous Galerkin methods for convection–diffusion problems with arbitrary Péclet number, in: *5th European Conference on Numerical Mathematics and Advanced Applications*, Prague, August 2003, Springer, 2000.

- [12] A. Buffa, T. J. Hughes, G. Sangalli, Analysis of a multiscale discontinuous Galerkin method for convection-diffusion problems, *SIAM Journal on Numerical Analysis* 44 (4) (2006) 1420–1440.
- [13] D. Schötzau, L. Zhu, A robust a-posteriori error estimator for discontinuous Galerkin methods for convection–diffusion equations, *Applied Numerical Mathematics* 59 (9) (2009) 2236–2255.
- [14] L. Zhu, D. Schötzau, A robust a posteriori error estimate for hp-adaptive DG methods for convection–diffusion equations, *IMA Journal of Numerical Analysis* 31 (3) (2011) 971–1005.
- [15] H. Chen, J. Li, W. Qiu, Robust a posteriori error estimates for HDG method for convection–diffusion equations, *IMA Journal of Numerical Analysis* 36 (1) (2016) 437–462.
- [16] G. Chen, M. Feng, X. Xie, A robust WG finite element method for convection–diffusion–reaction problems, *Journal of Computational and Applied Mathematics* 315 (2017) 107 – 125. doi:<https://doi.org/10.1016/j.cam.2016.10.029>.
URL <http://www.sciencedirect.com/science/article/pii/S0377042716305180>
- [17] R. Lin, X. Ye, S. Zhang, P. Zhu, A weak Galerkin Finite Element Method for Singularly Perturbed Convection-Diffusion-Reaction Problems, *SIAM Journal on Numerical Analysis* 56 (3) (2018) 1482–1497. arXiv:<https://doi.org/10.1137/17M1152528>, doi:10.1137/17M1152528.
URL <https://doi.org/10.1137/17M1152528>
- [18] J. Wang, X. Ye, A weak Galerkin finite element method for second-order elliptic problems, *J. Comput. Appl. Math.* 241 (2013) 103–115. doi:10.1016/j.cam.2012.10.003.
URL <http://dx.doi.org/10.1016/j.cam.2012.10.003>
- [19] K. Eriksson, C. Johnson, Adaptive streamline diffusion finite element methods for stationary convection-diffusion problems, *Mathematics of computation* 60 (201) (1993) 167–188.
- [20] R. Verfürth, Robust a posteriori error estimates for stationary convection-diffusion equations, *SIAM Journal on Numerical Analysis* 43 (4) (2005) 1766–1782.

- [21] R. Verfürth, A posteriori error estimators for convection-diffusion equations, *Numerische Mathematik* 80 (4) (1998) 641–663.
- [22] L. Tobiska, R. Verfürth, Robust a posteriori error estimates for stabilized finite element methods, *IMA Journal of Numerical Analysis* 35 (4) (2015) 1652–1671.
- [23] A. Ern, A. F. Stephansen, A posteriori energy-norm error estimates for advection-diffusion equations approximated by weighted interior penalty methods, *Journal of Computational Mathematics* (2008) 488–510.
- [24] A. Ern, A. F. Stephansen, M. Vohralík, Guaranteed and robust discontinuous Galerkin a posteriori error estimates for convection–diffusion–reaction problems, *Journal of Computational and Applied Mathematics* 234 (1) (2010) 114–130.
- [25] Q. H. Li, J. Wang, Weak Galerkin finite element methods for parabolic equations, *Numer. Methods Partial Differential Equations* 29 (6) (2013) 2004–2024.
- [26] J. Wang, X. Ye, A weak Galerkin finite element method for the Stokes equations, *Adv. Comput. Math.* 42 (1) (2016) 155–174.
doi:10.1007/s10444-015-9415-2.
URL <http://dx.doi.org/10.1007/s10444-015-9415-2>
- [27] L. Mu, J. Wang, X. Ye, A stable numerical algorithm for the Brinkman equations by weak Ga
J. Comput. Phys. 273 (2014) 327–342.
doi:10.1016/j.jcp.2014.04.017.
URL <http://dx.doi.org/10.1016/j.jcp.2014.04.017>
- [28] L. Mu, J. Wang, X. Ye, S. Zhang, A weak Galerkin finite element method for the Maxwell equations, *J. Sci. Comput.* 65 (1) (2015) 363–386.
doi:10.1007/s10915-014-9964-4.
URL <http://dx.doi.org/10.1007/s10915-014-9964-4>
- [29] L. Mu, J. Wang, X. Ye, Weak Galerkin finite element methods on polytopal meshes, *International Journal of Numerical Analysis and Modeling* 12 (1) (2015) 31–53.

- [30] L. Mu, J. Wang, Y. Wang, X. Ye, A weak Galerkin mixed finite element method for biharmonic equations, in: Numerical solution of partial differential equations: theory, algorithms, and their applications, Vol. 45 of Springer Proc. Math. Stat., Springer, New York, 2013, pp. 247–277. doi:10.1007/978-1-4614-7172-1_13. URL http://dx.doi.org/10.1007/978-1-4614-7172-1_13
- [31] L. Mu, J. Wang, X. Ye, Weak Galerkin finite element methods for the biharmonic equation on Numer. Methods Partial Differential Equations 30 (3) (2014) 1003–1029. doi:10.1002/num.21855. URL <http://dx.doi.org/10.1002/num.21855>
- [32] C. Wang, J. Wang, An efficient numerical scheme for the biharmonic equation by weak Galerkin Comput. Math. Appl. 68 (12, part B) (2014) 2314–2330. doi:10.1016/j.camwa.2014.03.021. URL <http://dx.doi.org/10.1016/j.camwa.2014.03.021>
- [33] C. Wang, J. Wang, A hybridized weak Galerkin finite element method for the biharmonic equation, Int. J. Numer. Anal. Model. 12 (2) (2015) 302–317.
- [34] L. Chen, J. Wang, X. Ye, A posteriori error estimates for weak Galerkin finite element methods for second order elliptic problems, Journal of Scientific Computing 59 (2) (2014) 496–511.
- [35] H. Li, A posteriori error estimates for the weak Galerkin finite element methods on polytopal meshes, Communications in Computational Physics 26 (2).
- [36] T. Zhang, Y. Chen, A posteriori error analysis for the weak Galerkin method for solving elliptic International Journal of Computational Methods 15 (08) (2018) 1850075. arXiv:<https://doi.org/10.1142/S0219876218500755>, doi:10.1142/S0219876218500755. URL <https://doi.org/10.1142/S0219876218500755>
- [37] J. H. Adler, X. Hu, L. Mu, X. Ye, An a posteriori error estimator for the weak Galerkin least-squares finite-element method 59 (2) (2018) 496–511.

- [38] X. Zheng, X. Xie, A posteriori error estimator for a weak Galerkin finite element solution of the Stokes problem, *East Asian Journal on Applied Mathematics* 7 (3) (2017) 508–529.
- [39] P. G. Ciarlet, *The finite element method for elliptic problems*, SIAM, 2002.
- [40] O. A. Karakashian, F. Pascal, A posteriori error estimates for a discontinuous Galerkin approximation of second-order elliptic problems, *SIAM Journal on Numerical Analysis* 41 (6) (2003) 2374–2399.
- [41] W. Bangerth, T. Heister, L. Heltai, G. Kanschat, M. Kronbichler, M. Maier, B. Turcksin, T. D. Young, *The deal.ii library, version 8.2. archive of numerical software*, *Archive of Numerical Software* 3.
- [42] W. Bangerth, R. Hartmann, G. Kanschat, *deal.ii – a general purpose object oriented finite element library.*, *ACM Trans. Math. Softw.* 33 (2007) 24/1–24/27.

